Published in final edited form as:
Brain Res. 2011 January 7; 1367: 146–161. doi:10.1016/j.brainres.2010.10.058.

Projections of the suprachiasmatic nucleus and ventral subparaventricular zone in the Nile grass rat *(Arvicanthis niloticus)*

Michael D. Schwartz[1,*], **Henryk F. Urbanski**[3], **Antonio A. Nunez**[1,2], and **Laura Smale**[1,2]

[1]Neuroscience Program, Michigan State University, East Lansing MI, 48824, USA

[2]Psychology Department, Michigan State University, East Lansing MI, 48824, USA

[3]Division of Neuroscience, Oregon Health and Science University, Beaverton, OR, 97006, USA

Abstract

The phases of many circadian rhythms differ between diurnal and nocturnal species. However, rhythms within the hypothalamic suprachiasmatic nucleus (SCN), which contains the central circadian pacemaker, are very similar, suggesting that the mechanisms underlying phase preference lie downstream of the SCN. Rhythms in Fos expression in the ventral subparaventricular zone (vSPVZ), a major target of the SCN, differ substantially between diurnal Nile grass rats and nocturnal lab rats, raising the possibility that the vSPVZ modulates the effects of SCN signals at its targets. To understand better how and where the SCN and vSPVZ communicate circadian signals within the grass rat brain, we mapped their projections using the anterograde tracer biotinylated dextran amine (BDA). Adult female grass rats received unilateral BDA injections directed at the SCN or vSPVZ and their brains were perfusion-fixed several days later. Immunohistochemistry revealed that the distribution patterns of SCN and vSPVZ efferents were very similar. Labeled fibers originating in each region were heavily concentrated in the medial preoptic area, paraventricular thalamic nucleus, the subparaventricular zone, and the hypothalamic paraventricular and dorsomedial nuclei. BDA-labeled fibers from the SCN and vSPVZ formed appositions with orexin neurons and gonadotropin-releasing hormone neurons, two cell populations whose rhythms in Fos expression track temporally reversed patterns of locomotor and reproductive behavior, respectively, in diurnal and nocturnal rodents. These data demonstrate that projections of the SCN and vSPVZ are highly conserved in diurnal and nocturnal rodents, and the vSPVZ projections may enable it to modulate the responsiveness of target cells to signals from the SCN.

Keywords

circadian rhythm; diurnality; suprachiasmatic nucleus; ventral subparaventricular zone; orexin; gonadotropin-releasing hormone

[*]Corresponding author (& present address): Michael D. Schwartz, Ph.D., Department of Pharmacology and Experimental Therapeutics, University of Maryland School of Medicine, 655 W Baltimore St. rm 4-027, Baltimore, MD 21201, Tel 410-706-5581, Fax 410-706-0032, mschw009@umaryland.edu[1].

Introduction

Circadian rhythms in behavior and physiology typically exhibit a species-specific diurnal, nocturnal or crepuscular pattern. In mammals, circadian rhythms are coordinated by a pacemaker located in the hypothalamic suprachiasmatic nucleus (SCN) (Moore and Eichler, 1972; Stephan and Zucker, 1972; Weaver, 1998). This structure appears to function in very similar ways in diurnal and nocturnal species, suggesting that the fundamental differences between them emerge from mechanisms downstream of the SCN (Mahoney et al., 2009; Smale et al., 2008). In fact, there is now direct evidence that this is the case for differences in glucocorticoid rhythms between diurnal *Arvicanthis ansorgeii* and nocturnal lab rats (Kalsbeek et al., 2008). A more complete understanding of the myriad features of diurnality, however, is hampered by a lack of information on where the SCN efferents project in day-active animals.

One region that may play an important role in mediation of diurnality is the hypothalamic subparaventricular zone (SPVZ), which extends dorsally and caudally from the SCN to the ventral edge of the hypothalamic paraventricular nucleus (PVN) (Paxinos and Watson, 2005). Not only is the SPVZ a major target of the SCN (Abrahamson and Moore, 2001; Kriegsfeld et al.; Moore and Leak, 2001; Watts et al., 1987), but also it has efferent projections to many of the same regions as the SCN in lab rats and hamsters (Morin et al., 1994; Orpen and Steiner, 1994; Watts and Swanson, 1987; Watts et al., 1987). Furthermore, multiple-unit activity (MUA) rhythms in the SPVZ are in phase with the locomotor activity rhythms of both diurnal and nocturnal rodents (Inouye and Kawamura, 1979; Sato and Kawamura, 1984), and in mice MUA rhythms re-entrain to a shifted LD cycle in parallel with the shifting locomotor activity rhythms (Nakamura et al., 2008). Finally, lesions in the ventral part of the SPVZ (vSPVZ) eliminate free-running circadian sleep-wake and locomotor rhythms in lab rats (R. norvegicus; Lu et al., 2001). Thus, the available functional and anatomical data from nocturnal rodents support a model whereby the SCN conveys circadian information to its targets both directly and indirectly via the SPVZ (Saper et al., 2005; Watts, 1991).

The vSPVZ may also play an important role in regulating rhythms in a diurnal rodent, the unstriped Nile grass rat (*Arvicanthis niloticus*; referred to here as “grass rats”). In these animals, which are day-active both in the lab and in the field (Blanchong et al., 1999; McElhinny et al., 1997), the vSPVZ (which we have referred to in previous reports as the lower subparaventricular zone [LSPV]) displays a rhythm in Fos immunoreactivity (Fos-ir) with a phase-relationship to the LD cycle that differs substantially from that seen in lab rats, and which persists in constant darkness (DD) in the former but not the latter species (Schwartz et al., 2004). The rhythmic Fos-ir population of cells is clearly outside the anatomical borders of the SCN and does not extend to the dorsal SPVZ (Nunez et al., 1999; Schwartz et al., 2004). While chemical lesions of the grass rat vSPVZ disrupt locomotor activity rhythms, they do not eliminate them, as is the case in lab rats (Schwartz et al., 2009). These data have led us to hypothesize that in grass rats, as in lab rats (Lu et al., 2001), rhythmic activity within the vSPVZ is important for shaping and maintaining circadian rhythms, and that differences in the vSPVZ’s activity may contribute to differences in the phase of physiological and behavioral rhythms in grass rats and lab rats, and perhaps in nocturnal and diurnal species more generally (Nunez et al., 1999; Schwartz et al., 2004; Schwartz et al., 2009). If this is the case, then signals from the vSPVZ should interact with those from the SCN, something that could occur at mutual target sites, and perhaps even in single cells that receive direct input from both the SCN and the vSPVZ. So far, however, efferent projections from the SCN and vSPVZ have not been described for a diurnal rodent species.

In the present study, we mapped the full extent of the projections of the grass rat SCN and vSPVZ using the anterograde tract tracer biotinylated dextran amine (BDA) and compared the distributions of fibers from these two areas. We then determined whether neurons in these regions project to two specific populations of cells that regulate circadian rhythms that are 180° out of phase in diurnal grass rats and nocturnal lab rats. Specifically, we looked at projections to cells containing gonadotropin-releasing hormone (GnRH) and those containing orexin-A (OXA) (Mahoney et al., 2004; Martinez et al., 2002; Martinez et al., 2009).

2. Results

2.1. Injection sites

Two injections were centered in the SCN (S1 & S2; Fig. 1A–F). Injection spread in S1 was entirely contained within the boundaries of the SCN (Fig. 1G), whereas S2 included a small amount of spread into the retrochiasmatic area. Four injections were centered in the vSPVZ (L1–L4; Fig. 1A–F). Cases L1 and L3 lay immediately adjacent to the dorsal and dorsolateral edges of the mid- to caudal SCN and extended outwards up to 400 μm from its borders (Fig. 1H), overlapping entirely with the distribution of Fos-positive cells in the vSPVZ (Fig. 1, hatched area; Schwartz et al., 2004). In Case L2 the center was slightly rostral to those of L1 and L3, but there was significant overlap. The center of the injection site in Case L4 was farthest from the SCN and, although the spread overlapped with the vSPVZ, it extended well beyond this area both dorsally and laterally. Of these four injections, L1 was the smallest and L4 the largest. None of the four injections centered in the vSPVZ labeled cells in the SCN as revealed by neutral red counterstaining in alternate sections. Cases S1 and L1, representative hits in the SCN and vSPVZ respectively, are described in more detail, with descriptions of the other cases included when they differ.

2.2. Injections centered in the SCN

Following injections centered in the SCN, BDA-labeled fibers were most dense in the periventricular and medial hypothalamus, parts of the basal and limbic forebrain, and a few thalamic targets (Fig. 2). Fibers usually displayed varicosities and exhibited moderate to heavy branching. This pattern was nearly identical in cases S1 and S2, with slightly increased fiber density overall in S2 compared to S1.

Rostrally-directed BDA-ir fibers coursed along the edge of the optic chiasm, through the medial preoptic area (mPOA) and the periventricular nucleus to terminate in the diagonal band of Broca, the organum vasculosum of the lamina terminalis (OVLT) and the lateral septum (Fig. 2A–E, Fig. 4A). The ventrolateral and lateral preoptic areas were lightly innervated. Fibers were often thick in the mPOA, whereas more dorsally-directed fibers were thin and exhibited few branches or varicosities until reaching their terminal fields in the medial, ventral, and to a lesser extent, the intermediate lateral septal nuclei.

Laterally-directed fibers coursed along the optic chiasm to the borders of the supraoptic nucleus. The majority of these fibers terminated there, but a few fibers followed the optic tract to the intergeniculate leaflet (IGL). These fibers were thin, unbranched and had few varicosities until reaching their terminal field in the IGL, where varicosities were abundant (Fig. 4B). This was the most bilateral of all the labeled pathways, with nearly identical fiber densities in the ipsilateral and contralateral IGL. A few fibers were seen in the medial amygdala close to the optic tract in S2 but not in S1.

Dorsally-projecting fibers ran caudal to the anterior commissure to innervate densely the anterior paraventricular thalamus (PVT), the parataenial nucleus, and medial aspects of the bed nuclei of the stria terminalis (BNST; Fig. 2E–G). More fibers were present in medial

divisions of the bed nuclei in S2 than in S1, and neither case exhibited fibers in the oval nucleus of the BNST. The contralateral PVT was moderately innervated. A few fibers also continued caudally to innervate moderately the mid- and posterior PVT (Fig.2H–I).

A large dorsocaudal projection extended from the SCN into the SPVZ (Fig. 2G–K). Adjacent to the SCN, these fibers overlapped the vSPVZ area where Fos, particularly at night, and calbindin are heavily concentrated in the grass rat (Schwartz et al.). This plexus continued through the SPVZ to the PVN (Fig.2I–K). Many terminals were evident within the dorsal SPVZ, as well as the periventricular and dorsal parvocellular compartments of the PVN; fewer fibers were present in the medial parvocellular PVN, and only sparse fibers were seen in the magnocellular PVN (Fig. 6A). A few fibers continued dorsally to the medial zona incerta (Fig.2J–K), but many more ran caudally to the dorsomedial hypothalamic nucleus (DMH; Fig.2M–P). Fibers were concentrated in the pars compacta of the DMH though all parts of the DMH were innervated (Fig. 2N–O; Fig 5B). Dorsal to the DMH, thin spindle-like fibers ran dorsocaudally through the periventricular gray to the habenula (Fig.2N–P). BDA-ir fibers also coursed caudally through the retrochiasmatic area and ventral tuberal hypothalamus, providing moderate input to the anterior hypothalamic, perifornical and lateral hypothalamus (Fig.2L–O). Labeled fibers surrounded the area dorsal and medial to the ventromedial hypothalamic nucleus, with some fibers penetrating the nucleus itself (Fig. 2L–N, Fig. 5C). Fibers extended as far caudally as the dorsal tuberomammillary nucleus.

2.3. Injections centered in the vSPVZ

The distribution of BDA-ir fibers following injections into the vSPVZ was quite similar to that described following injections into the SCN. However, vSPVZ projections tended to be more evenly distributed along the medial-lateral axis of the hypothalamus than were SCN efferents, which were more concentrated in the medial and periventricular zones.

Anterior to the SCN, fibers extended rostrally from the vSPVZ to innervate the preoptic area, diagonal band of Broca and lateral septum (Fig. 3A–E). Labeled fibers were observed in the ventromedial, ventrolateral and medial preoptic nuclei, as well as the anteroventral periventricular nucleus. The vSPVZ projection to the septum was about as dense as that of the SCN, whereas innervation of the mPOA was lighter (Fig. 2, 3).

A small group of fibers coursed laterally along the optic chiasm to the supraoptic nucleus (Fig. 3G). In cases L1 and L3, where injections were centered squarely in the vSPVZ, there were a few scattered fibers in the amygdala (Fig. 3J–K), whereas more rostral injections (L2 and L4) resulted in greater numbers of labeled fibers. The medial amygdalar nucleus was the only part of the amygdala with BDA-ir fibers in all four cases of injections into the vSPVZ. Because the increased innervation of the amygdala was associated with more rostrally-centered injections, at least some of these fibers are likely to have originated in the caudal preoptic area or anterior hypothalamus rather than the vSPVZ.

In cases L1 and L4, a few fibers were visible in the IGL (Fig. 4E), but none were observed in L2 and L3. Given the overlaps in location of injections L1, L2 and L3, and the fact that larger injections (L2, L3) did not label fibers in the IGL, it is not possible to confirm a projection from the vSPVZ to the IGL. The injection site for L4 extended further laterally than L1 – L3, into the anterior hypothalamic area; it is thus possible that the fibers seen in this case could have arisen from this region. We cannot rule out the possibility that a small amount of tracer crossed into the SCN in L1, as both L2 and L3 were larger injections that also extended up to the border of the SCN, but did not yield BDA-ir fibers in the IGL.

Dorsally-projecting fibers innervated the anterior PVT (Fig.3F–G); these were longer and thinner than those emanating from the SCN. Fibers also extended into medial aspects of the BNST anterior to the PVT, but did not enter the oval nucleus of the BNST (Fig.3E). Fibers in the PVT were less dense than those seen following injections into the SCN, whereas fibers in the BNST were slightly denser.

The majority of vSPVZ fibers extended caudally through the SPVZ (Fig. 3H–J). A few fibers were seen in the caudal parvocellular PVN (Fig. 5D), spreading out laterally and avoiding magnocellular cell bodies. Innervation of the medial zona incerta was denser than that seen following SCN injections (Fig.3J–L). These fibers were far more extensive in cases L3 and L4 than in L1, whereas in L2 no fibers were seen in the zona incerta or dorsal to the PVN, and magnocellular paraventricular neurons were heavily interweaved by BDA-ir fibers. Fibers extending caudally and laterally from the SPVZ, PVN and zona incerta lightly (L1 and L3) to moderately (L2 and L4) innervated the perifornical region (Fig.3L–N). In the DMH, the overall density of labeled fibers was lower after injections into the vSPVZ than the SCN, but the pars compacta region had many labeled fibers in cases with injections in either the SCN or the vSPVZ (Fig. 3L–N, Fig. 5E). Fibers continued dorsally and caudally past the DMH to terminate in the posterior hypothalamic area, periventricular gray and the habenula (Fig.3N–O).

A ventral group of fibers proceeded caudally from the vSPVZ along the basal edge of the hypothalamus to the retrochiasmatic and anterior hypothalamic areas (Fig.3I–J). Further caudally, these fibers surrounded the ventromedial hypothalamic nucleus, the ventral tuberal region lateral to it and the perifornical region (Fig. 3L–N). In contrast to SCN projections, fibers from the vSPVZ were dense within the ventromedial nucleus, particularly in the central and ventrolateral subregions (Fig. 5F). Further caudally, fibers continued into the dorsal and ventral tuberomammillary nuclei, and gradually decreased in density until the end of the mammillary recess of the third ventricle, when they were no longer seen.

2.4. GnRH-ir neurons and BDA-ir fibers

The morphology and the distribution of GnRH neurons in the forebrain were similar to those previously reported for female grass rats (Mahoney and Smale, 2005a; McElhinny et al., 1999). BDA-ir fibers following injections into both the SCN and vSPVZ were interspersed with GnRH-ir neurons at all rostrocaudal levels, but were most dense in and around the OVLT and the adjacent POA. BDA-ir fibers with varicosities displayed apparent terminal boutons and en passant appositions on GnRH-ir cell bodies (Fig. 6A and 6B–E respectively). The proportion of GnRH neurons with putative appositions was substantial in all cases; these appositions were concentrated in the OVLT and the POA/SCN following injections centered in either the SCN or the vSPVZ (Table 1). BDA-ir fibers more frequently exhibited appositions with GnRH neurons ipsilateral to injections in either the SCN or vSPVZ; however, many appositions were observed contralateral to the injection sites, and were more common following injections in the SCN than in the vSPVZ (Table 1). BDA-ir fibers with varicosities were also frequently in apparent apposition to GnRH-ir processes at some distance from the cell body (not shown). These putative fiber-fiber contacts were present throughout the OVLT and adjacent POA and were seen following SCN and vSPVZ injections.

2.5. OXA-ir neurons and BDA-ir fibers

OXA neurons in the perifornical hypothalamus exhibited similar morphology and distributions to those previously reported for grass rats (Martinez et al., 2002; Nixon and Smale, 2004). BDA-ir fibers with varicosities were in very close proximity to OXA-ir cell bodies and displayed putative appositions following injections centered in the SCN and the

vSPVZ (Fig. 7A–D). In addition, many BDA-ir fibers with varicosities from the SCN and vSPVZ were also observed in apparent apposition with OXA-ir processes as described above for GnRH-ir neurons. (not shown).

Following BDA injections into the SCN, more putative appositions with OXA neurons were seen in the medial and central divisions than in the lateral division (Table 2). The percentage of cells with appositions in these areas was substantially elevated in case S2 compared to S1, although their distribution was similar across the three rostro-caudal levels and featured a strong ipsilatersal bias in both cases. Following injections centered in the vSPVZ, putative appositions with OXA neurons were fewer than in the two SCN cases, and were concentrated in the medial and central divisions with a clear ipsilateral bias (Table 2). In cases L2 and L4 putative appositions were more concentrated in the central and lateral divisions than in cases L1 and L3,in which they were heavily concentrated in the medial division.

3. Discussion

3.1. Summary of findings

The efferent projections of the SCN and vSPVZ of the grass rat, like those of nocturnal lab rats, exhibited a largely overlapping distribution of terminal sites in the hypothalamus, limbic forebrain and midline thalamus. The overlap of projections extended to two cell groups, GnRH and OXA neurons, in which rhythmic activity is reversed in diurnal grass rats compared to nocturnal lab rats. The similarity of SCN and vSPVZ efferent projections to those of other nocturnal rodents suggests that the neural basis for a diurnal or nocturnal phase preference is likely to reside in functional differences, rather than structural ones, within elements of the circadian timing system and its associated outputs.

3.2. Some caveats

The vSPVZ is of special interest in grass rats because of the temporal pattern of Fos expressed within it. Although that Fos expression can be systematically assessed using a sampling box, the region where it is seen is not circumscribed by a clearly defined nuclear boundary (Schwartz et al., 2004). Rather, that Fos expression, which rises in the mid-subjective night, fans out from the SCN and its concentration decreases as the distance from the SCN increases; cells containing calbindin are likewise distributed across the same region in the same manner, but again, do not sharply define it (Schwartz et al., 2004). Consequently, the exact location of the vSPVZ injection sites in the present study, relative to the distribution of markers such as Fos, is open to interpretation. Nevertheless, it is clear that injections L1–L4 each successfully deposited BDA into part or all of the region of interest, and comparisons across these cases permit an informative assessment of its projections. The vSPVZ's innermost boundary- between its ventral aspect and the SCN- is clearly delineated in Nissl- and Neutral Red- stained sections (Schwartz et al., 2004); while care was taken to select only cases in which the tracer injection did not cross this boundary, we recognize the possibility that a small, nearly undetectable amount of tracer could have spread from the vSPVZ into the SCN, or vice versa. A second caveat is that our results do not enable us to determine whether projections of the different subregions of the SCN differ in grass rats, as they do in lab rats and hamsters (Kriegsfeld et al.; Leak and Moore, 2001). On the other hand, these data are the first, to our knowledge, to characterize the efferent projections of the SCN and vSPVZ in a diurnal species. These results thus provide an important guide for future studies using retrograde tracers to characterize in detail the phenotype and projection patterns of cells within the vSPVZ and SCN subregions. Finally, because sex differences within the SCN have been documented in grass rats and other species (Dardente et al., 2004;

Krajnak et al., 1998; Mahoney et al., 2009), future studies will be needed to determine if the results from our female study pertain also to males.

3.3. General output pathways of the SCN and vSPVZ

Most projections from the SCN and vSPVZ were seen within the hypothalamus, particularly in its medial and periventricular zones. However, direct projections to hypothalamic areas that mediate sleep/wake behavior, such as the ventrolateral preoptic area and median preoptic nucleus, were sparse. The circadian system may influence sleep/wake state primarily through its projections to the mPOA, SPVZ and DMH (Deurveilher and Semba, 2004; Saper et al., 2005) and to OXA producing neurons (see below) that in turn project to many brain regions that support wakefulness (Mintz et al., 2001; Nixon and Smale, 2007; Novak and Albers, 2002; Ohno and Sakurai, 2008). In lab rats the mPOA, SPVZ and DMN are extensively interconnected (Deurveilher et al., 2002; Deurveilher and Semba, 2003; Deurveilher and Semba, 2004; Gu and Simerly, 1997; Simerly and Swanson, 1986; Simerly and Swanson, 1988; ter Horst and Luiten, 1986; Thompson et al., 1996; Thompson and Swanson, 1998; Watts and Swanson, 1987; Watts et al., 1987), and they project to regions more directly involved in sleep/wake state (e.g. the ventrolateral preoptic area (Deurveilher et al., 2002), median preoptic nucleus (Deurveilher and Semba, 2003) tuberomammillary nuclei, and OXA neurons (Deurveilher and Semba, 2004)). In both lab rats and grass rats, the SCN and vSPVZ may influence sleep/wake state, and perhaps other behaviors, through their projections to this integrative network (Swanson, 2000), though their effects on these systems is likely to be quite different.

The extrahypothalamic target that received the most input from the SCN and vSPVZ was the PVT. A dense plexus of fibers that were labeled following BDA injections into each of these regions was seen throughout the entire rostrocaudal extent of the PVT. In lab rats the projections between the SCN and PVT are reciprocal, and these nuclei have several hypothalamic targets in common (Moga et al., 1995). However, the PVT also sends major ascending fibers to several telencephalic regions, including the amygdala and the cerebral cortex (Moga et al., 1995), which may represent the most direct route through which SCN signals could reach these areas (Sylvester et al., 2002). The PVT is a primary target of the SCN signaling molecule prokineticin 2, whose mRNA exhibits rhythms that are strikingly similar in the SCN of mice and grass rats (Cheng et al., 2002; Lambert et al., 2005); daily Fos rhythms in the PVT are also quite similar in these two species (Novak and Nunez, 1998; Novak et al., 2000). These patterns raise the possibility that cells within the PVT of grass rats and nocturnal rodents respond in the same ways to input from the SCN and/or vSPVZ, which may not be the case for cells in other hypothalamic regions that have been examined (reviewed in Smale et al., 2008).

The IGL differed from other target regions in that labeled fibers were abundant there following all SCN injections, but only sparse following some vSPVZ injections, and absent in others. In hamsters (Morin et al., 1992; Vidal et al., 2005; Vrang et al., 2003) and lab rats (Card and Moore, 1989; Moore and Card, 1994) retrograde tracers injected into the IGL label small numbers of cell bodies in and around the SCN and large numbers of cells in the retrochiasmatic area, and anterograde tracer injections into the SCN and vSPVZ each labeled fibers in the IGL (Kriegsfeld et al., 2004; Morin et al., 1994; Watts et al., 1987). In the present study, although IGL cells were consistently labeled when injections were centered in the SCN, this was not the case when the tracer was deposited in vSPVZ. The SCN is both functionally and anatomically complex (Morin et al., 2006), and such heterogeneity may also exist in the tissue surrounding it (Ramanathan et al., 2006). Retrograde tracing will be necessary to determine exactly which cells within and around the SCN project to the IGL.

3.4. Projections from the SCN and vSPVZ to GnRH- and OXA-ir neurons

The parallelism seen in SCN and vSPVZ efferents extended to two discrete populations of cells, those containing OXA and GnRH, respectively. This is of special interest as these cells undergo daily patterns of Fos production that are reversed in grass rats relative to nocturnal rodents (Mahoney and Smale, 2005a; Martinez et al., 2002; Martinez et al., 2009). The arousal-promoting orexin neurons (Espana et al., 2001; Lee et al., 2005; Scammell et al., 2000) represent one way for circadian cues to interface with the sleep-wake system noted above (Deboer et al., 2004; Espana et al., 2001; Zeitzer et al., 2003), and they project to widespread regions of the brain in grass rats as well as lab rats (Nixon and Smale, 2007). The SCN projects to orexin neurons in rats (Abrahamson et al., 2001; but see Sakurai et al., 2005; Yoshida et al., 2006), and here we found numerous appositions between BDA-ir fibers emanating from both the SCN and the vSPVZ. The SCN, but not the vSPVZ, exhibited a substantial number of appositions with OXA neurons contralateral to the injection site. We interpret this to reflect a contralateral projection from the injected SCN; while we cannot rule out a small leakage of tracer into the contralateral SCN, we did not observe any evidence for this in the injections sites.

Direct projections from the SCN to hypothalamic GnRH-containing cells have also been seen in lab rats and hamsters and are thought to play a role in the circadian gating of the LH surge in these species (de la Iglesia et al., 1995; de la Iglesia and Schwartz, 2006; van der Beek et al., 1993; Van der Beek et al., 1997). The ovulatory surge in LH (McElhinny et al., 1999) and Fos expression within GnRH neurons, both occur at opposite times of day in grass rats and these nocturnal rodents (Mahoney et al., 2004). In the case of the GnRH cell rhythm, the pattern persists when grass rats and lab rats are housed in constant darkness for several days. The present evidence that fibers originating in both the SCN and vSPVZ could form appositions with GnRH cells suggests that these structures may play roles in the generation and/or modulation of rhythms in them. Appositions with GnRH neurons were observed both ipsilateral and contralateral to injection sites in the SCN and the vSPVZ, suggesting that in grass rats, the vSPVZ projects more widely to GnRH neurons than it does to OXA neurons (in which contralateral appositions from the vSPVZ were rare).

Taken together, the current data on OXA and GnRH neurons support the idea that target cells may respond differently to circadian signals emanating directly from the SCN in diurnal and nocturnal species. These findings are also consistent with the hypothesis that the vSPVZ could play a role in generation and/or regulation of rhythms in these cells.

3.5. Functional Implications

While the SCN and the vSPVZ of both diurnal and nocturnal species appear to project to essentially the same target areas, several lines of evidence suggest that vSPVZ outputs may differ functionally from those of the SCN in at least two respects. First, the two structures are likely to release a different set of signaling molecules, as a variety of neuropeptides present in the SCN are absent in the vSPVZ. These include, for example, vasopressin and vasoactive intestinal polypeptide (Abrahamson and Moore, 2001; Moore and Silver, 1998; Smale and Boverhof, 1999; Watts and Swanson, 1987), both of which are contained in fibers emanating from the SCN (Abrahamson and Moore, 2001; Mahoney and Smale, 2005a; Van der Beek et al., 1997), and which play roles in regulation of neuroendocrine rhythms (Kriegsfeld and Silver, 2006). A second difference between the grass rat SCN and vSPVZ is that they exhibit different patterns of rhythmicity at the cellular level. When grass rats are kept on a light-dark cycle Fos expression increases in the vSPVZ within 5 hours of lights-off, but not in the SCN until lights-on (Nunez et al., 1999; Schwartz et al., 2004). These differences in the temporal patterns of activity, and in the chemical signals used, suggest that

in grass rats, the vSPVZ is more than a relay for SCN signals. Rather, the SCN and vSPVZ may send distinctly different signals to their common targets.

Although the grass rat vSPVZ and SCN are different with respect to cell phenotypes and their patterns of rhythmicity, they are similar in other respects. In both regions, Fos rhythms are endogenous (Schwartz et al., 2004) and are buffered against major changes in activity state (Schwartz and Smale, 2005). Rhythmic activity in the grass rat vSPVZ, like that within the SCN, is therefore not dependent on a light-dark cycle and is not heavily influenced by sleep/wake state or behavioral arousal. Signals coming from the vSPVZ are thus likely to be more tightly coupled to the pacemaker than to many features of the external environment or to internal state. Both the SCN and the vSPVZ express daily rhythms in expression of the clock gene products Per1 and Per2 (Ramanathan et al., 2006). The observation that the vSPVZ projects to nearly all of the same regions as the SCN provides further support for the idea that it plays an important timekeeping role in these animals.

3.6. Conclusions

Although the function of the vSPVZ is not fully understood in either diurnal or nocturnal species, in lab rats it appears to be involved in regulating the timing of both reproduction-related events (Arendash and Gallo, 1979; Docke et al., 1982; Fernandez-Galaz et al., 1999; Watts et al., 1989) and locomotor activity (Lu et al., 2001; Moore and Danchenko, 2002). However, circadian body temperature rhythms persist with reduced amplitudes in animals with ventral sPVZ lesions (Lu et al., 2001), suggesting that, although the ventral sPVZ may be necessary for expression of some rhythmic processes, it is not essential for all. In grass rats chemotoxic lesions of the vSPVZ impair activity rhythms and increase the ratio of nighttime to daytime activity (Schwartz et al., 2009). In grass rats, the vSPVZ displays an endogenous rhythm in Fos expression that is 8 hours advanced relative to that in the SCN, whereas in lab rats, this rhythm is in phase with the SCN rhythm under a light-dark cycle and does not persist in constant dark conditions (Schwartz et al., 2004). Thus, rhythmic activity in the grass rat vSPVZ is different from both the activity of its own SCN, and from the activity of the vSPVZ of nocturnal lab rats. The clear parallelism in the efferent anatomy of the SCN and vSPVZ in grass rats demonstrated in the current study is consistent with the hypothesis that projections from these two regions may converge on common targets. If this is the case, then signals from the vSPVZ could alter the responses of these cells to signals originating in the SCN, and perhaps do this differently in diurnal grass rats compared to nocturnal species such as lab rats.

4. Experimental Procedure

4.1. Animals

Adult female grass rats (n=6) obtained from a breeding colony at Michigan State University (Katona and Smale, 1997) were singly housed in Plexiglas cages (34 × 28 × 17 cm) with access to food (PMI Nutrition Prolab RMH 2000, Brentwood, MO) and water *ad libitum*. Animals were kept in a 12:12 light:dark cycle; a red light (<5 lux) remained on constantly for animal care purposes. Female grass rats were used for injections because circadian rhythms in GnRH activity in female grass rats were correlated with the ovulatory LH surge and female reproductive behavior (Mahoney et al., 2004; Mahoney and Smale, 2005b). Grass rats exhibit a postpartum estrus rather than a spontaneous ovulatory cycle as lab rats do (McElhinny et al., 1997), as least as reflected by cyclic changes in vaginal cytology. For that reason estrous phase was not monitored in these individuals. All experiments were approved by, and performed in compliance with, guidelines established by the Michigan State University All-University Committee on Animals Use and Care, and the National Research Council’s Guide for the Care and Use of Laboratory Animals.

4.2. Surgical Procedures and tissue collection

All animals received a unilateral iontophoretic injection of 10,000 MW BDA (Molecular Probes; Eugene, OR) directed at the SCN or vSPVZ. Animals were deeply anesthetized with sodium pentobarbital (50 mg/kg i.p.) prior to surgery, and then the head was shaved, wiped with betadine, and injected with lidocaine (0.03 mL s.c.). Animals were placed into a stereotaxic apparatus (Stoelting Co.; Wood Dale, IL) with the incisor bar set to −6.0 mm and the micropipette set at an angle of 10 degrees, and a 1–2 cm incision was made in the scalp to expose the skull. Injection coordinates were: 1.4 mm anterior to bregma, 1.2 mm lateral to bregma, and 6.3 mm ventral to the dura. A small hole was drilled in the skull and dura was gently broken to allow uninterrupted passage of the micropipette. A glass micropipette (WPI; Sarasota, FL) with inner tip diameter of 10–15 μm was then filled with 10% BDA in 0.01 M phosphate-buffered saline (PBS; pH 7.4) and lowered slowly to injection depth. Injections were made under 5 mA positive alternating current (7 sec on/ 7 sec off) for 7 minutes, followed by a 7-minute rest period. Micropipettes were then withdrawn slowly under negative current. The incision was closed with autoclips, and animals were given 0.06 mL buprenorphine i.m. and 1.0 mL sterile saline s.c. Seven days later, animals were given an overdose of sodium pentobarbital and perfused transcardially with 0.01M phosphate-buffered saline (PBS), pH 7.2, followed by 4% paraformaldehyde (Sigma, St. Louis, MO) in 0.1M phosphate buffer. Brains were post-fixed for 4 hours, and then transferred to 20% sucrose solution overnight. Brains were sectioned coronally at 30 μm on a freezing microtome into 3 series of sections, which were then stored in cryoprotectant at −20°C until processing began.

4.3. Immunohistochemistry

One series of free-floating sections was rinsed 3 × 10 minutes in PBS at room temperature, and then incubated in avidin-biotin complex (ABC Vectastain Kit, Vector Laboratories, Burlingame, CA). ABC complex was visualized by reacting with diaminobenzidine (0.5 mg/mL; Sigma) in Trizma buffer (Sigma) enhanced with nickel sulfate. Tissue was mounted, dehydrated, and coverslipped with Permount. An alternate series from each animal with a successful injection was reacted as above, mounted and counterstained with neutral red to assist in mapping brain regions. Injections were considered successful if they were centered on, and restricted to, either the SCN or the vSPVZ.

A third series from each successful injection was processed for double-labeling of BDA and GnRH (sections rostral to and including SCN) or BDA and OXA (sections caudal to SCN). Unless noted otherwise, incubations were conducted at room temperature for 1 h on a shaker, and tissue was rinsed 3 × 10 min in PBS between incubations. Free-floating sections were first processed for BDA-ir as described above. Sections were then rinsed in PBS and incubated in i) 5% normal serum in PBS with 0.3% Triton X-100, ii) primary antibody for 48 h at 4 °C, iii) biotinylated secondary antibody (1:200) and iv) ABC. Protein was visualized by reacting sections with diaminobenzidine (0.5 mg/mL; Sigma) in Trizma buffer (Sigma). Sections were then mounted, dehydrated, and coverslipped with Permount. Reagents used for GnRH included: i) 5% normal horse serum (Vector), ii) mouse anti-GnRH (1:5000; HU4H antibody characterized in Urbanski, 1991), iii) biotinylated horse anti-mouse (1:200; Vector). Reagents used for OXA included: i) 5% normal donkey serum (Jackson Laboratories, Bar Harbor, ME), ii) goat anti OXA (Santa Cruz Biochemistry, Santa Cruz, CA), iii) biotinylated donkey anti-goat (1:200; Jackson). Specificity of labeling was previously verified (Nixon and Smale, 2004; Urbanski, 1991). Primary deletion controls for each peptide resulted in absence of stain (not shown).

4.4. Microscopy

Sections were analyzed on a Zeiss Axioskop microscope (Zeiss, Germany) under brightfield illumination, and all photomicrographs were taken using a Zeiss Axiocam MR (Zeiss) and adjusted for brightness and contrast in Adobe Photoshop 7.0 (Adobe Systems; Mountain View, CA). The full extent of labeled fibers was mapped from two representative cases (SCN: S1, vSPVZ: L1). Fibers were traced in Photoshop using a drawing pad (Wacom; Vancouver, WA) from a series of photomicrographs taken at 10×; these were then combined in Photoshop to form a composite image of the section. Although BDA can be carried in a retrograde direction (Reiner et al., 2000), we saw very few BDA-ir cell bodies that were not associated with the injection sites. All anatomical landmarks and nuclear boundaries were drawn from neutral-red stained sections adjacent to those from which labeled fibers were mapped; structures in these sections were identified using a rat brain atlas (Paxinos and Watson, 1998; Paxinos and Watson, 2005)}.

Appositions of BDA-ir fibers with GnRH or OXA neurons were evaluated under bright-field illumination using a 100× oil immersion lens. GnRH-ir neurons with and without BDA-ir appositions (also referred to as contacts) were counted in 3 rostrocaudal zones encompassing the MS and DBB (6 sections), the OVLT (2 sections), and the POA and SON (6 sections). OXA-ir neurons with and without BDA-ir appositions were counted bilaterally in three sections using a 1200 × 700 μm box divided into thirds and aligned with one side against the third ventricle and the bottom of the box aligned with the ventral border of the fornix (Martinez et al., 2002). A neuron was considered to be contacted by a BDA-ir fiber if, in the same plane of focus, a swelling on a BDA-ir axon (blue-black fiber) was observed abutting a GnRH- or OXA-ir cell body (brown cell), or a labeled primary process emanating from a GnRH- or OXA-ir cell body.

Research Highlights

- The SCN projects to the midline hypothalamus and thalamus in grass rats.
- The grass rat vSPVZ is a major SCN target whose projections parallel those of the the SCN.
- SCN and vSPVZ fibers contact orexin-A and gonadotropin-releasing hormone neurons.
- Phase reversal of circadian rhythms in the vSPVZ may modulate responses to SCN signals in diurnal rodents.

Acknowledgments

The authors wish to thank Dr. Sharleen Sakai, and Anna Baumgras for technical assistance.

Supported by National Institute of Health grants MH53433 to LS, HD29186 to HFU, and MH070087 to MDS

Abbreviations

BDA	biotinylated dextran amine
BNST	bed nuclei of the stria terminalis
DD	constant darkness
DMH	dorsomedial hypothalamic nucleus

GnRH	gonadotropin-releasing hormone
IGL	intergeniculate leaflet
LSPV	lower subparventricular zone
mPOA	medial preoptic area
MUA	multiple unit activity
OVLT	organum vasculosum of the lamina terminalis
OXA	orexin A
PVN	paraventricular hypothalamic nucleus
PVT	paraventricular thalamic nucleus
SCN	suprachiasmatic nucleus
SPVZ	subparaventricular zone
vSPVZ	ventral subparaventricular zone

References

Abrahamson EE, Leak RK, Moore RY. The suprachiasmatic nucleus projects to posterior hypothalamic arousal systems. Neuroreport. 2001; 12:435–440. [PubMed: 11209963]

Abrahamson EE, Moore RY. Suprachiasmatic nucleus in the mouse: retinal innervation, intrinsic organization and efferent projections. Brain Res. 2001; 916:172–191. [PubMed: 11597605]

Arendash GW, Gallo RV. Regional differences in response to electrical stimulation within the medial preoptic-suprachiasmatic region on blood luteinizing hormone levels in ovariectomized and ovariectomized, estrogen-primed rats. Endocrinology. 1979; 104:333–343. [PubMed: 446364]

Blanchong JA, McElhinny TL, Mahoney MM, Smale L. Nocturnal and diurnal rhythms in the unstriped Nile rat, Arvicanthis niloticus. J Biol Rhythms. 1999; 14:364–377. [PubMed: 10511004]

Card JP, Moore RY. Organization of lateral geniculate-hypothalamic connections in the rat. J Comp Neurol. 1989; 284:135–147. [PubMed: 2754028]

Cheng MY, Bullock CM, Li C, Lee AG, Bermak JC, Belluzzi J, Weaver DR, Leslie FM, Zhou QY. Prokineticin 2 transmits the behavioural circadian rhythm of the suprachiasmatic nucleus. Nature. 2002; 417:405–410. [PubMed: 12024206]

Dardente H, Menet JS, Challet E, Tournier BB, Pevet P, Masson-Pevet M. Daily and circadian expression of neuropeptides in the suprachiasmatic nuclei of nocturnal and diurnal rodents. Brain Res Mol Brain Res. 2004; 124:143–151. [PubMed: 15135222]

de la Iglesia HO, Blaustein JD, Bittman EL. The suprachiasmatic area in the female hamster projects to neurons containing estrogen receptors and GnRH. Neuroreport. 1995; 6:1715–1722. [PubMed: 8541467]

de la Iglesia HO, Schwartz WJ. Minireview: timely ovulation: circadian regulation of the female hypothalamo-pituitary-gonadal axis. Endocrinology. 2006; 147:1148–1153. [PubMed: 16373412]

Deboer T, Overeem S, Visser NAH, Duindam H, Frolich M, Lammers GJ, Meijer JH. Convergence of circadian and sleep regulatory mechanisms on hypocretin-1. Neuroscience. 2004; 129:727–732. [PubMed: 15541893]

Deurveilher S, Burns J, Semba K. Indirect projections from the suprachiasmatic nucleus to the ventrolateral preoptic nucleus: a dual tract-tracing study in rat. Eur J Neurosci. 2002; 16:1195–1213. [PubMed: 12405980]

Deurveilher S, Semba K. Indirect projections from the suprachiasmatic nucleus to the median preoptic nucleus in rat. Brain Res. 2003; 987:100–106. [PubMed: 14499951]

Deurveilher S, Semba K. Indirect projections from the suprachiasmatic nucleus to major arousal-promoting cell groups in rat: Implications for the circadian control of behavioural state. Neuroscience. 2004; 130:165–183. [PubMed: 15561433]

Docke F, Lung DN, Rohde W, Dorner G. Perisuprachiasmatic lesions enhance the increase of gonadotropin secretion in acutely ovariectomized rats. Endokrinologie. 1982; 79:311–314. [PubMed: 6813111]

Espana RA, Baldo BA, Kelley AE, Berridge CW. Wake-promoting and sleep-suppressing actions of hypocretin (orexin): basal forebrain sites of action. Neuroscience. 2001; 106:699–715. [PubMed: 11682157]

Fernandez-Galaz MC, Martinez Munoz R, Villanua MA, Garcia-Segura LM. Diurnal oscillation in glial fibrillary acidic protein in a perisuprachiasmatic area and its relationship to the luteinizing hormone surge in the female rat. Neuroendocrinology. 1999; 70:368–376. [PubMed: 10567863]

Gu GB, Simerly RB. Projections of the sexually dimorphic anteroventral periventricular nucleus in the female rat. J Comp Neurol. 1997; 384:142–164. [PubMed: 9214545]

Inouye ST, Kawamura H. Persistence of circadian rhythmicity in a mammalian hypothalamic "island" containing the suprachiasmatic nucleus. Proc Natl Acad Sci U S A. 1979; 76:5962–5966. [PubMed: 293695]

Kalsbeek A, Verhagen LA, Schalij I, Foppen E, Saboureau M, Bothorel B, Buijs RM, Pevet P. Opposite actions of hypothalamic vasopressin on circadian corticosterone rhythm in nocturnal versus diurnal species. Eur J Neurosci. 2008; 27:818–827. [PubMed: 18279365]

Katona C, Smale L. Wheel-running rhythms in Arvicanthis niloticus. Physiol Behav. 1997; 61:365–372. [PubMed: 9089754]

Krajnak K, Kashon ML, Rosewell KL, Wise PM. Sex differences in the daily rhythm of vasoactive intestinal polypeptide but not arginine vasopressin messenger ribonucleic acid in the suprachiasmatic nuclei. Endocrinology. 1998; 139:4189–4196. [PubMed: 9751499]

Kriegsfeld LJ, Leak RK, Yackulic CB, LeSauter J, Silver R. Organization of suprachiasmatic nucleus projections in Syrian hamsters (Mesocricetus auratus): an anterograde and retrograde analysis. J Comp Neurol. 2004; 468:361–379. [PubMed: 14681931]

Kriegsfeld LJ, Silver R. The regulation of neuroendocrine function: Timing is everything. Horm Behav. 2006; 49:557–574. [PubMed: 16497305]

Lambert CM, Machida KK, Smale L, Nunez AA, Weaver DR. Analysis of the prokineticin 2 system in a diurnal rodent, the unstriped Nile grass rat (Arvicanthis niloticus). J Biol Rhythms. 2005; 20:206–218. [PubMed: 15851527]

Leak RK, Moore RY. Topographic organization of suprachiasmatic nucleus projection neurons. J Comp Neurol. 2001; 433:312–334. [PubMed: 11298358]

Lee MG, Hassani OK, Jones BE. Discharge of identified orexin/hypocretin neurons across the sleep-waking cycle. J Neurosci. 2005; 25:6716–6720. [PubMed: 16014733]

Lu J, Zhang YH, Chou TC, Gaus SE, Elmquist JK, Shiromani P, Saper CB. Contrasting effects of ibotenate lesions of the paraventricular nucleus and subparaventricular zone on sleep-wake cycle and temperature regulation. J Neurosci. 2001; 21:4864–4874. [PubMed: 11425913]

Mahoney MM, Sisk C, Ross HE, Smale L. Circadian regulation of gonadotropin-releasing hormone neurons and the preovulatory surge in luteinizing hormone in the diurnal rodent, Arvicanthis niloticus, and in a nocturnal rodent, Rattus norvegicus. Biol Reprod. 2004; 70:1049–1054. [PubMed: 14668212]

Mahoney MM, Smale L. Arginine vasopressin and vasoactive intestinal polypeptide fibers make appositions with gonadotropin-releasing hormone and estrogen receptor cells in the diurnal rodent Arvicanthis niloticus. Brain Res. 2005a; 1049:156–164. [PubMed: 15936731]

Mahoney MM, Smale L. A daily rhythm in mating behavior in a diurnal murid rodent Arvicanthis niloticus. Horm Behav. 2005b; 47:8–13. [PubMed: 15579260]

Mahoney MM, Ramanathan C, Hagenauer MH, Thompson RC, Smale L, Lee T. Daily rhythms and sex differences in vasoactive intestinal polypeptide, VIPR2 receptor and arginine vasopressin mRNA in the suprachiasmatic nucleus of a diurnal rodent, Arvicanthis niloticus. Eur J Neurosci. 2009; 30:1537–1543. [PubMed: 19811536]

Martinez GS, Smale L, Nunez AA. Diurnal and nocturnal rodents show rhythms in orexinergic neurons. Brain Res. 2002; 955:1–7. [PubMed: 12419515]

Martinez GS, Schwartz MD, Smale L, Nunez AA. Circadian regulation of daily rhythms in orexinergic neurons in diurnal and nocturnal rodents. Revista Latinoamericana De Psicologia. 2009; 41:13–25.

McElhinny TL, Smale L, Holekamp KE. Patterns of body temperature, activity, and reproductive behavior in a tropical murid rodent, Arvicanthis niloticus. Physiol Behav. 1997; 62:91–96. [PubMed: 9226347]

McElhinny TL, Sisk CL, Holekamp KE, Smale L. A morning surge in plasma luteinizing hormone coincides with elevated Fos expression in gonadotropin-releasing hormone-immunoreactive neurons in the diurnal rodent, Arvicanthis niloticus. Biol Reprod. 1999; 61:1115–1122. [PubMed: 10491652]

Mintz EM, van den Pol AN, Casano AA, Albers HE. Distribution of hypocretin-(orexin) immunoreactivity in the central nervous system of Syrian hamsters (Mesocricetus auratus). J Chem Neuroanat. 2001; 21:225–238. [PubMed: 11382534]

Moga MM, Weis RP, Moore RY. Efferent projections of the paraventricular thalamic nucleus in the rat. J Comp Neurol. 1995; 359:221–238. [PubMed: 7499526]

Moore RY, Eichler VB. Loss of a circadian adrenal corticosterone rhythm following suprachiasmatic lesions in the rat. Brain Res. 1972; 42:201–206. [PubMed: 5047187]

Moore RY, Card JP. Intergeniculate leaflet: an anatomically and functionally distinct subdivision of the lateral geniculate complex. J Comp Neurol. 1994; 344:403–430. [PubMed: 8063960]

Moore RY, Silver R. Suprachiasmatic nucleus organization. Chronobiol Int. 1998; 15:475–487. [PubMed: 9787937]

Moore, RY.; Leak, RK. Suprachiasmatic Nucleus. In: Takahashi, JS.; Turek, FW.; Moore, RY., editors. Handbook of Behavioral Neurobiology, Vol. 12: Circadian Clocks. Handbook of Behavioral Neurobiology, Vol. 12. New York: Kluwer Academic/Plenum Publishers; 2001. p. 141-179.

Moore RY, Danchenko RL. Paraventricular-subparaventricular hypothalamic lesions selectively affect circadian function. Chronobiol Int. 2002; 19:345–360. [PubMed: 12025929]

Morin LP, Blanchard J, Moore RY. Intergeniculate leaflet and suprachiasmatic nucleus organization and connections in the golden hamster. Vis Neurosci. 1992; 8:219–230. [PubMed: 1372173]

Morin LP, Goodless-Sanchez N, Smale L, Moore RY. Projections of the suprachiasmatic nuclei, subparaventricular zone and retrochiasmatic area in the golden hamster. Neuroscience. 1994; 61:391–410. [PubMed: 7526267]

Morin LP, Shivers KY, Blanchard JH, Muscat L. Complex organization of mouse and rat suprachiasmatic nucleus. Neuroscience. 2006; 137:1285–1297. [PubMed: 16338081]

Nakamura W, Yamazaki S, Nakamura TJ, Shirakawa T, Block GD, Takumi T. In vivo monitoring of circadian timing in freely moving mice. Curr Biol. 2008; 18:381–385. [PubMed: 18334203]

Nixon JP, Smale L. Individual differences in wheel-running rhythms are related to temporal and spatial patterns of activation of orexin A and B cells in a diurnal rodent (*Arvicanthis niloticus*). Neuroscience. 2004; 127:25–34. [PubMed: 15219665]

Nixon JP, Smale L. A comparative analysis of the distribution of immunoreactive orexin A and B in the brains of nocturnal and diurnal rodents. Behav Brain Funct. 2007; 3:28. [PubMed: 17567902]

Novak CM, Nunez AA. Daily rhythms in Fos activity in the rat ventrolateral preoptic area and midline thalamic nuclei. Am J Physiol. 1998; 275:R1620–R1626. [PubMed: 9791082]

Novak CM, Smale L, Nunez AA. Rhythms in Fos expression in brain areas related to the sleep-wake cycle in the diurnal Arvicanthis niloticus. Am J Physiol Regul Integr Comp Physiol. 2000; 278:R1267–R1274. [PubMed: 10801296]

Novak CM, Albers HE. Localization of hypocretin-like immunoreactivity in the brain of the diurnal rodent, Arvicanthis niloticus. J Chem Neuroanat. 2002; 23:49–58. [PubMed: 11756009]

Nunez AA, Bult A, McElhinny TL, Smale L. Daily rhythms of Fos expression in hypothalamic targets of the suprachiasmatic nucleus in diurnal and nocturnal rodents. J Biol Rhythms. 1999; 14:300–306. [PubMed: 10447310]

Ohno K, Sakurai T. Orexin neuronal circuitry: role in the regulation of sleep and wakefulness. Front Neuroendocrinol. 2008; 29:70–87. [PubMed: 17910982]

Orpen BG, Steiner M. Neural connections of the suprachiasmatic nucleus and medial hypothalamus of the Syrian hamster (Mesocricetus auratus). J Anat. 1994; 184(Pt 1):23–33. [PubMed: 8157491]

Paxinos, G.; Watson, C. The rat brain in stereotaxic coordinates. Vol. Vol.. San Diego: Academic Press; 1998.

Paxinos, G.; Watson, C. The rat brain in stereotaxic coordinates. Vol. Vol. Boston: Elsevier Academic Press, Amsterdam; 2005.

Ramanathan C, Nunez AA, Martinez GS, Schwartz MD, Smale L. Temporal and spatial distribution of immunoreactive PER1 and PER2 proteins in the suprachiasmatic nucleus and peri-suprachiasmatic region of the diurnal grass rat (Arvicanthis niloticus). Brain Res. 2006; 1073–1074:348–358.

Reiner A, Veenman CL, Medina L, Jiao Y, Del Mar N, Honig MG. Pathway tracing using biotinylated dextran amines. J Neurosci Methods. 2000; 103:23–37. [PubMed: 11074093]

Sakurai T, Nagata R, Yamanaka A, Kawamura H, Tsujino N, Muraki Y, Kageyama H, Kunita S, Takahashi S, Goto K, Koyama Y, Shioda S, Yanagisawa M. Input of orexin/hypocretin neurons revealed by a genetically encoded tracer in mice. Neuron. 2005; 46:297–308. [PubMed: 15848807]

Saper CB, Lu J, Chou TC, Gooley J. The hypothalamic integrator for circadian rhythms. Trends Neurosci. 2005; 28:152–157. [PubMed: 15749169]

Sato T, Kawamura H. Circadian rhythms in multiple unit activity inside and outside the suprachiasmatic nucleus in the diurnal chipmunk (Eutamias sibiricus). Neurosci Res. 1984; 1:45–52. [PubMed: 6543592]

Scammell TE, Estabrooke IV, McCarthy MT, Chemelli RM, Yanagisawa M, Miller MS, Saper CB. Hypothalamic arousal regions are activated during modafinil-induced wakefulness. J Neurosci. 2000; 20:8620–8628. [PubMed: 11069971]

Schwartz MD, Nunez AA, Smale L. Differences in the suprachiasmatic nucleus and lower subparaventricular zone of diurnal and nocturnal rodents. Neuroscience. 2004; 127:13–23. [PubMed: 15219664]

Schwartz MD, Smale L. Individual differences in rhythms of behavioral sleep and its neural substrates in nile grass rats. J Biol Rhythms. 2005; 20:526–537. [PubMed: 16275771]

Schwartz MD, Nunez AA, Smale L. Rhythmic cFos expression in the ventral subparaventricular zone influences general activity rhythms in the Nile grass rat, Arvicanthis niloticus. Chronobiol Int. 2009; 26:1290–1306. [PubMed: 19916832]

Simerly RB, Swanson LW. The organization of neural inputs to the medial preoptic nucleus of the rat. J Comp Neurol. 1986; 246:312–342. [PubMed: 3517086]

Simerly RB, Swanson LW. Projections of the medial preoptic nucleus: a Phaseolus vulgaris leucoagglutinin anterograde tract-tracing study in the rat. J Comp Neurol. 1988; 270:209–242. [PubMed: 3259955]

Smale L, Boverhof J. The suprachiasmatic nucleus and intergeniculate leaflet of Arvicanthis niloticus, a diurnal murid rodent from East Africa. J Comp Neurol. 1999; 403:190–208. [PubMed: 9886043]

Smale L, Nunez AA, Schwartz MD. Rhythms in a diurnal brain. Biological Rhythm Research. 2008; 39:305–318.

Stephan FK, Zucker I. Circadian rhythms in drinking behavior and locomotor activity of rats are eliminated by hypothalamic lesions. Proc Natl Acad Sci U S A. 1972; 69:1583–1586. [PubMed: 4556464]

Swanson LW. Cerebral hemisphere regulation of motivated behavior. Brain Res. 2000; 886:113–164. [PubMed: 11119693]

Sylvester CM, Krout KE, Loewy AD. Suprachiasmatic nucleus projection to the medial prefrontal cortex: a viral transneuronal tracing study. Neuroscience. 2002; 114:1071–1080. [PubMed: 12379260]

ter Horst GJ, Luiten PG. The projections of the dorsomedial hypothalamic nucleus in the rat. Brain Res Bull. 1986; 16:231–248. [PubMed: 3697791]

Thompson RH, Canteras NS, Swanson LW. Organization of projections from the dorsomedial nucleus of the hypothalamus: a PHA-L study in the rat. J Comp Neurol. 1996; 376:143–173. [PubMed: 8946289]

Thompson RH, Swanson LW. Organization of inputs to the dorsomedial nucleus of the hypothalamus: a reexamination with Fluorogold and PHAL in the rat. Brain Res Brain Res Rev. 1998; 27:89–118. [PubMed: 9622601]

Urbanski HF. Monoclonal antibodies to luteinizing hormone-releasing hormone: production, characterization, and immunocytochemical application. Biol Reprod. 1991; 44:681–686. [PubMed: 2043738]

van der Beek EM, Wiegant VM, van der Donk HA, van den Hurk R, Buijs RM. Lesions of the suprachiasmatic nucleus indicate the presence of a direct vasoactive intestinal polypeptide-containing projection to gonadotrophin-releasing hormone neurons in the female rat. J Neuroendocrinol. 1993; 5:137–144. [PubMed: 8485548]

Van der Beek EM, Horvath TL, Wiegant VM, Van den Hurk R, Buijs RM. Evidence for a direct neuronal pathway from the suprachiasmatic nucleus to the gonadotropin-releasing hormone system: combined tracing and light and electron microscopic immunocytochemical studies. J Comp Neurol. 1997; 384:569–579. [PubMed: 9259490]

Vidal L, Blanchard J, Morin LP. Hypothalamic and zona incerta neurons expressing hypocretin, but not melanin concentrating hormone, project to the hamster intergeniculate leaflet. Neuroscience. 2005; 134:1081–1090. [PubMed: 15994022]

Vrang N, Mrosovsky N, Mikkelsen JD. Afferent projections to the hamster intergeniculate leaflet demonstrated by retrograde and anterograde tracing. Brain Res Bull. 2003; 59:267–288. [PubMed: 12464399]

Watts AG, Swanson LW. Efferent projections of the suprachiasmatic nucleus: II. Studies using retrograde transport of fluorescent dyes and simultaneous peptide immunohistochemistry in the rat. J Comp Neurol. 1987; 258:230–252. [PubMed: 2438309]

Watts AG, Swanson LW, Sanchez-Watts G. Efferent projections of the suprachiasmatic nucleus: I. Studies using anterograde transport of Phaseolus vulgaris leucoagglutinin in the rat. J Comp Neurol. 1987; 258:204–229. [PubMed: 3294923]

Watts AG, Sheward WJ, Whale D, Fink G. The effects of knife cuts in the sub-paraventricular zone of the female rat hypothalamus on oestrogen-induced diurnal surges of plasma prolactin and LH, and circadian wheel-running activity. J Endocrinol. 1989; 122:593–604. [PubMed: 2769171]

Watts, AG. The efferent projections of the suprachiasmatic nucleus: anatomical insights into the control of circadian rhythms. In: Klein, DC.; Moore, RY.; Reppert, SM., editors. Suprachiasmatic Nucleus: The Mind's Clock. Vol. Vol. New York: Oxford University Press; 1991. p. 77-106.

Weaver DR. The suprachiasmatic nucleus: a 25-year retrospective. J Biol Rhythms. 1998; 13:100–112. [PubMed: 9554572]

Yoshida K, McCormack S, Espana RA, Crocker A, Scammell TE. Afferents to the orexin neurons of the rat brain. J Comp Neurol. 2006; 494:845–861. [PubMed: 16374809]

Zeitzer JM, Buckmaster CL, Parker KJ, Hauck CM, Lyons DM, Mignot E. Circadian and homeostatic regulation of hypocretin in a primate model: implications for the consolidation of wakefulness. J Neurosci. 2003; 23:3555–3560. [PubMed: 12716965]

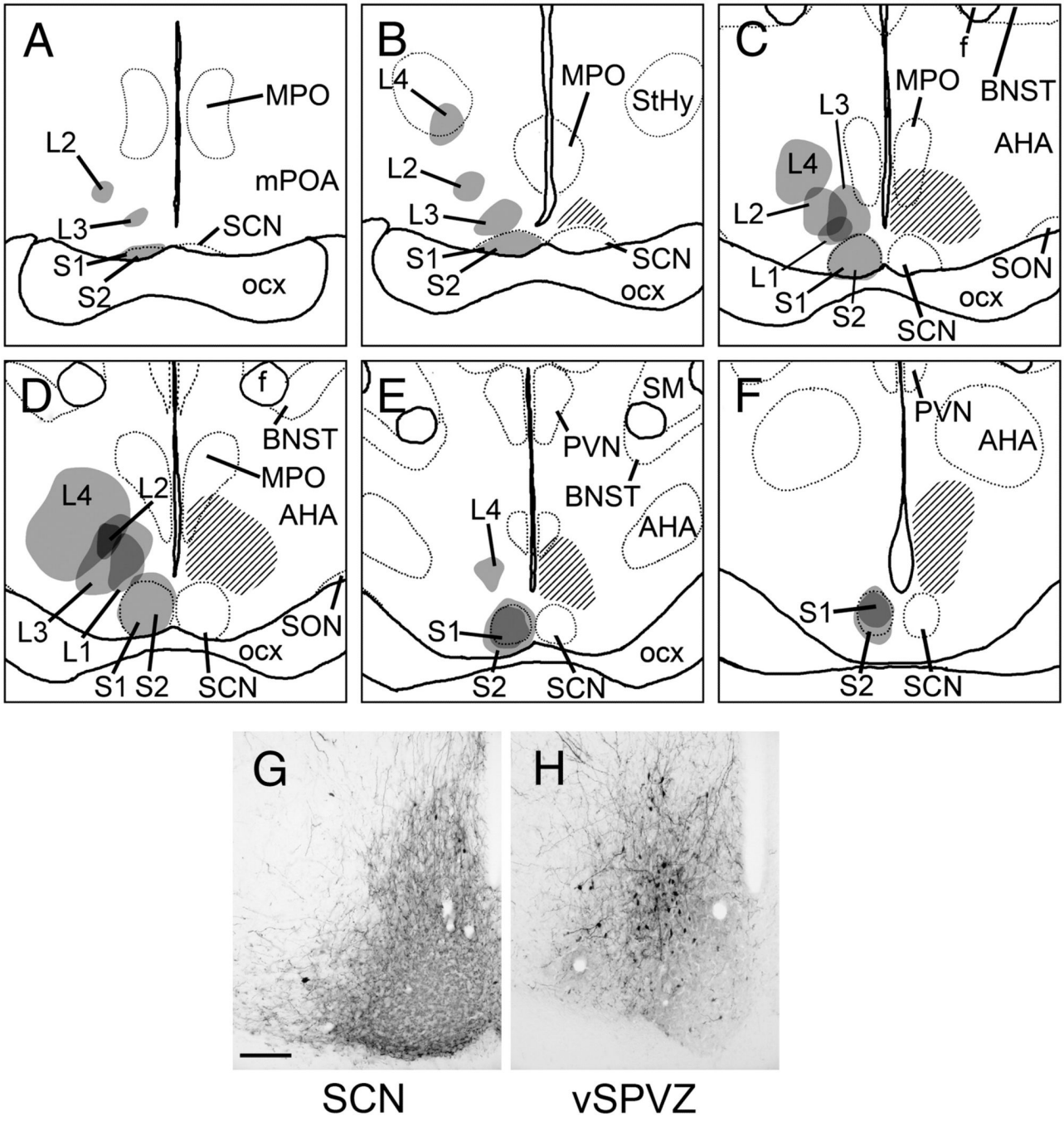

Figure 1.

A–F, Line drawings depicting the location of BDA injections in all cases described in the present study. Panels are arranged rostral-to-caudal, and were traced from sections as described in text. Gray shaded areas indicate center of tracer deposit; darker shading represents overlap between multiple cases. Cross-hatched area in each panel indicates the distribution of Fos-immunoreactive cells in the late night as determined by previous studies (adapted from Schwartz et al, 2004), and is included as a reference to indicate the vSPVZ region of interest that was targeted for injections. Dotted lines represent boundaries of selected brain structures as visualized by neutral red counterstain. G–H, representative photomicrographs of BDA injections centered in the SCN (G; case S1) and vSPVZ (H, case

L3). Scale bar = 100 μm. AHA, anterior hypothalamic area; BNST, bed nucleus of the stria terminalis; f, fornix; MPO, medial preoptic nucleus; mPOA, medial preoptic area; optic chiasm, optic chiasm; PVN, hypothalamic paraventricular nucleus; SCN, suprachiasmatic nucleus; SM, stria medullaris; SON, supraoptic nucleus; StHy, striohypothalamic nucleus.

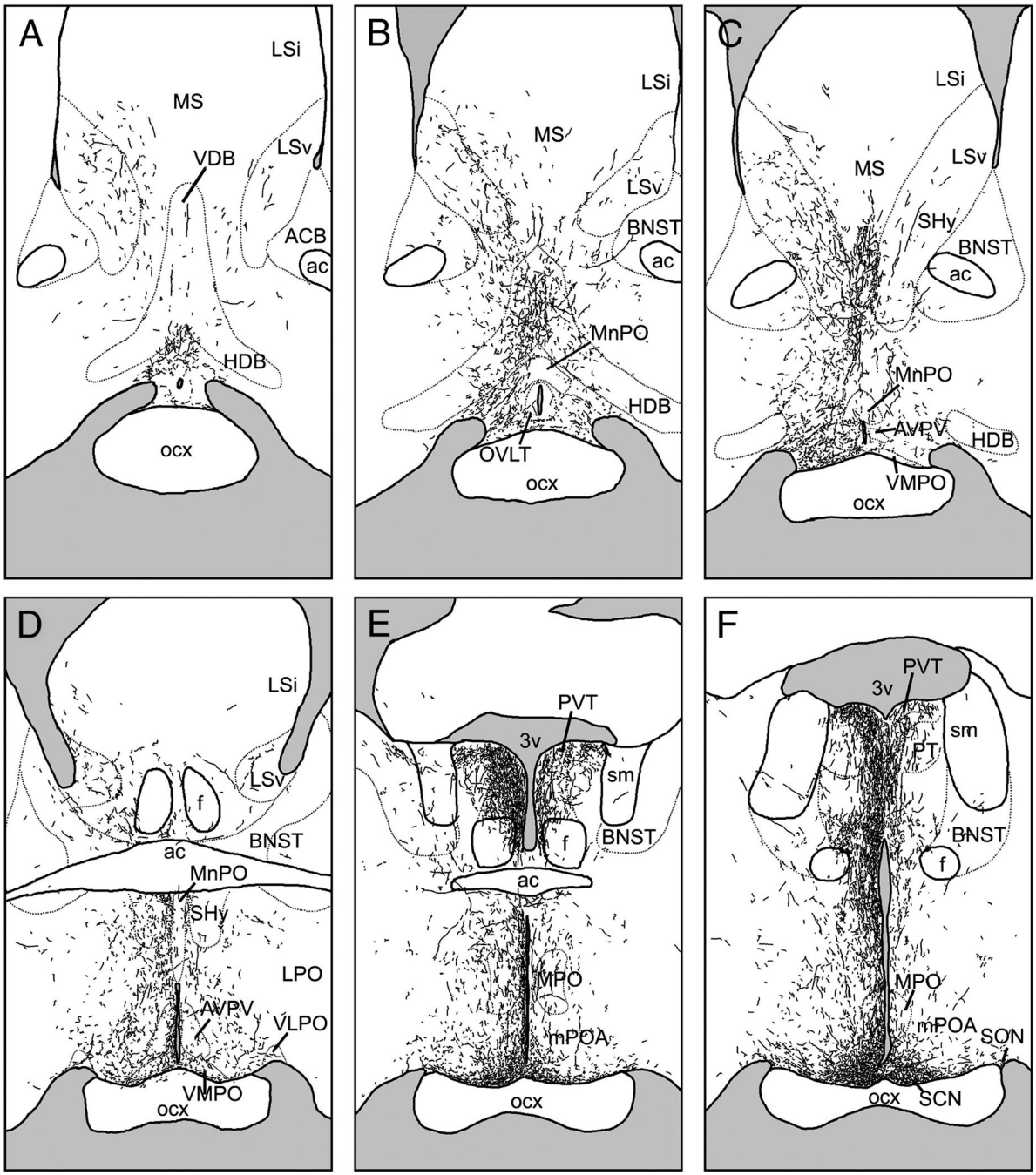

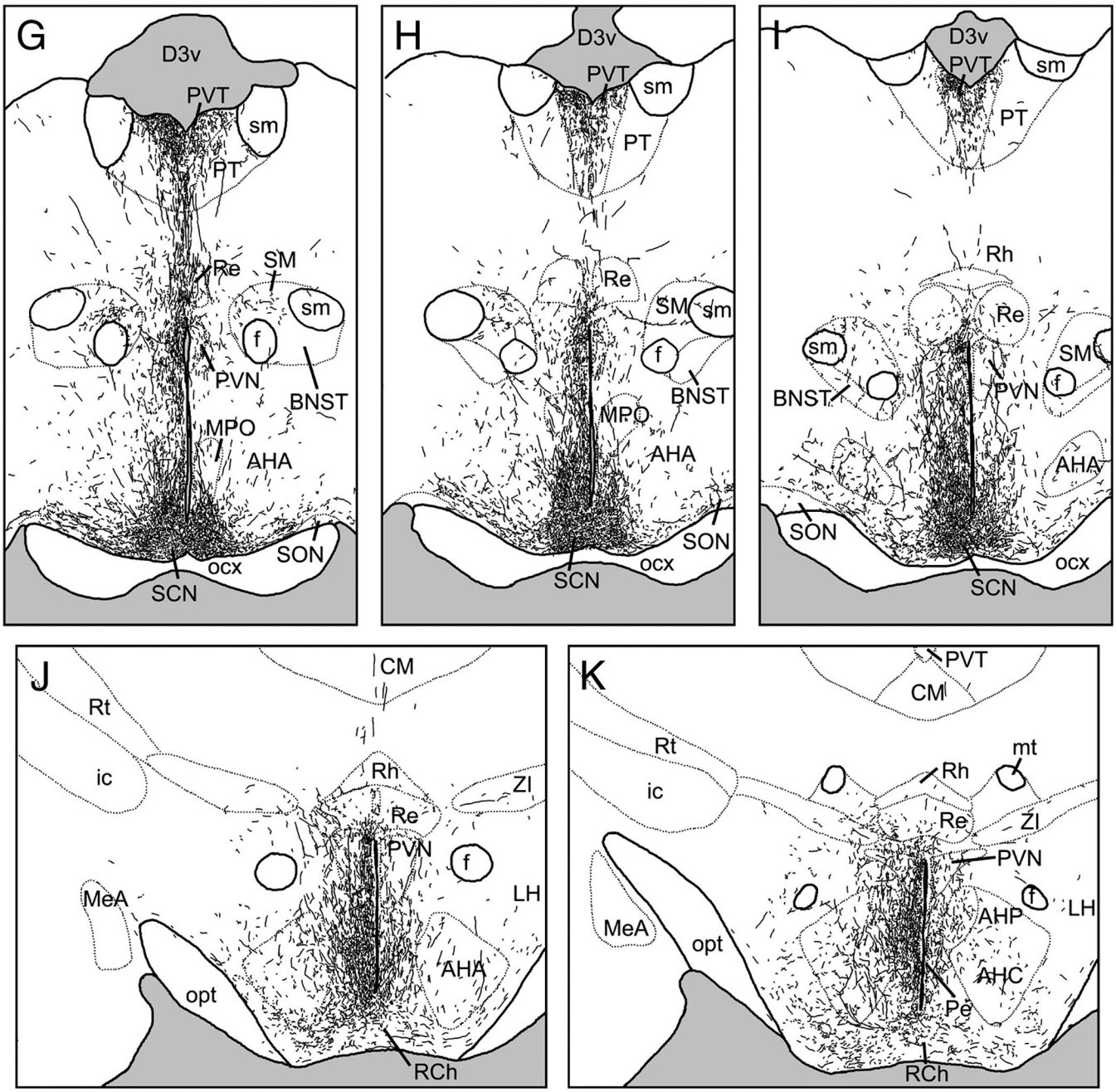

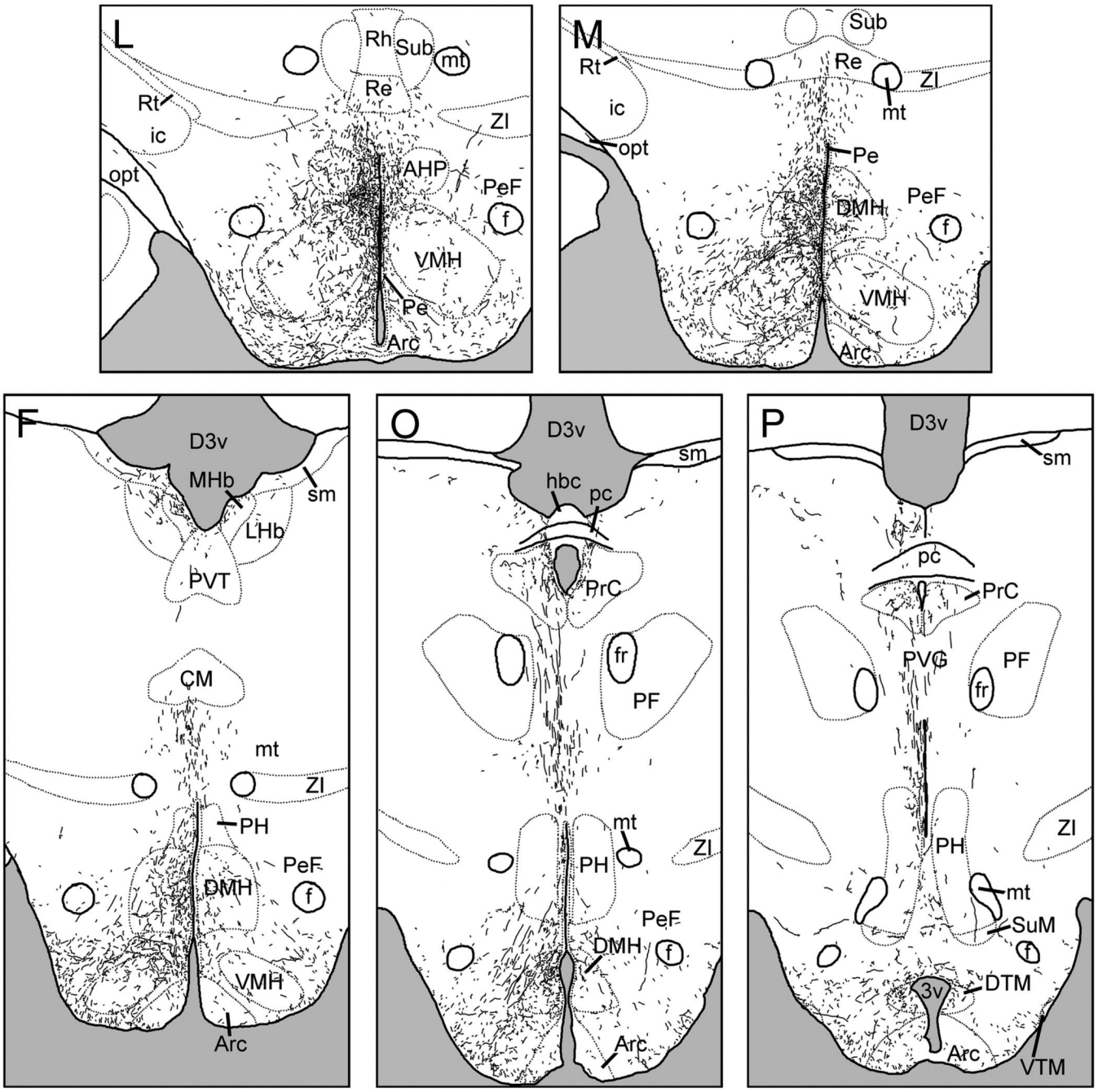

Figure 2.

Line drawings depicting the distribution of BDA-labeled fibers following an injection centered in the suprachiasmatic nucleus (SCN; case S1). Panels are arranged rostral-to-caudal, and were traced from sections as described in text. See Table 1 for abbreviations.

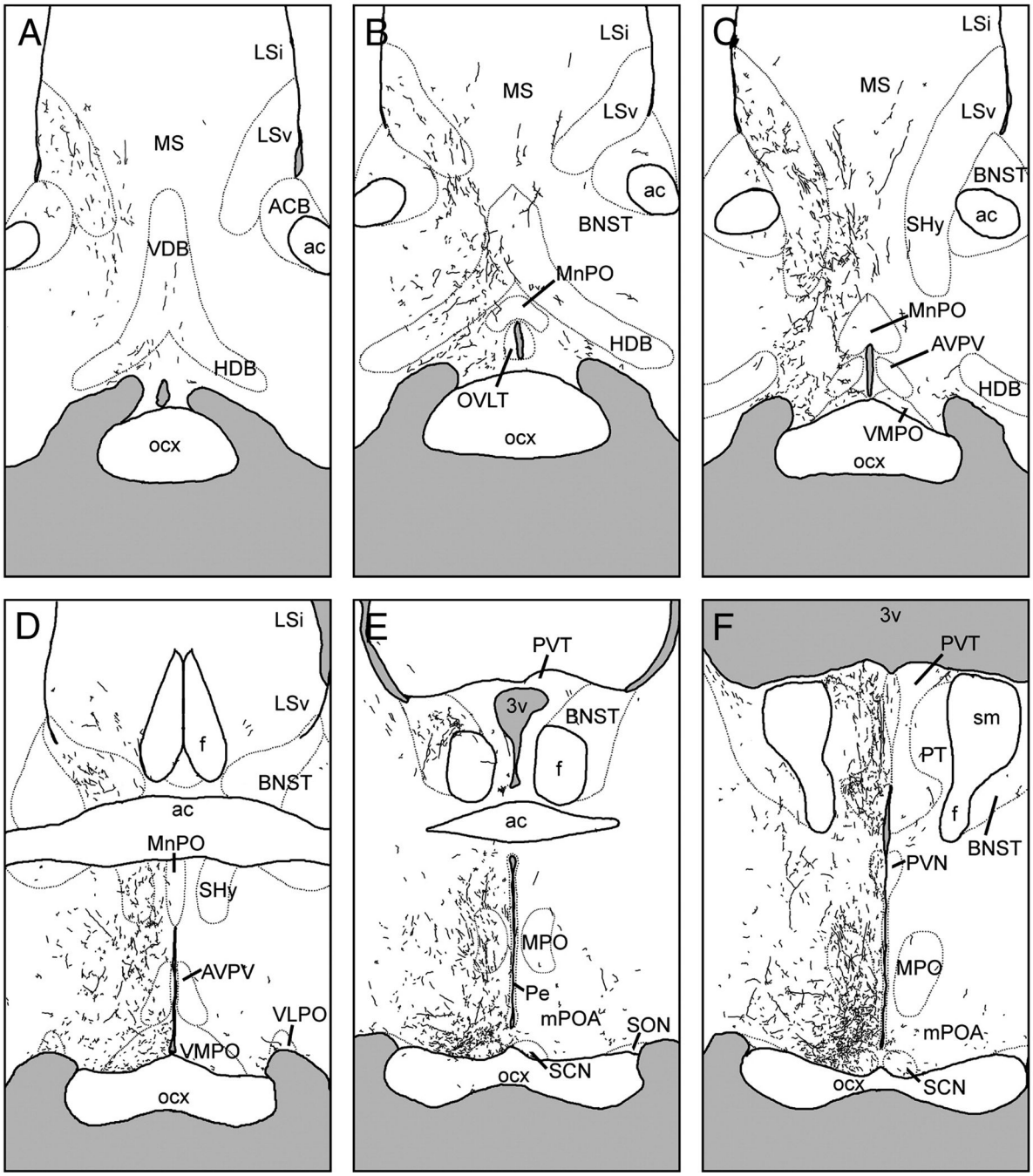

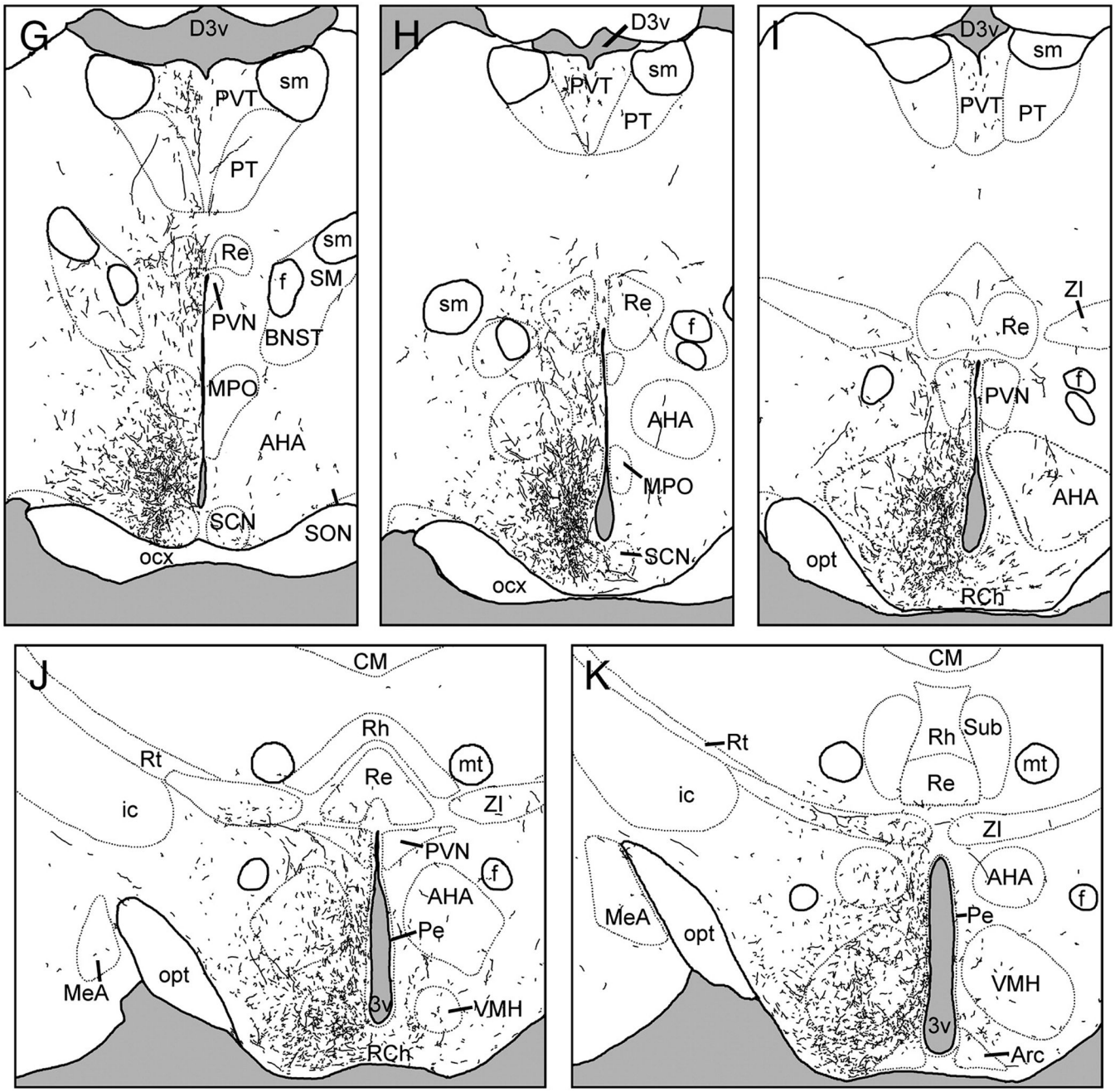

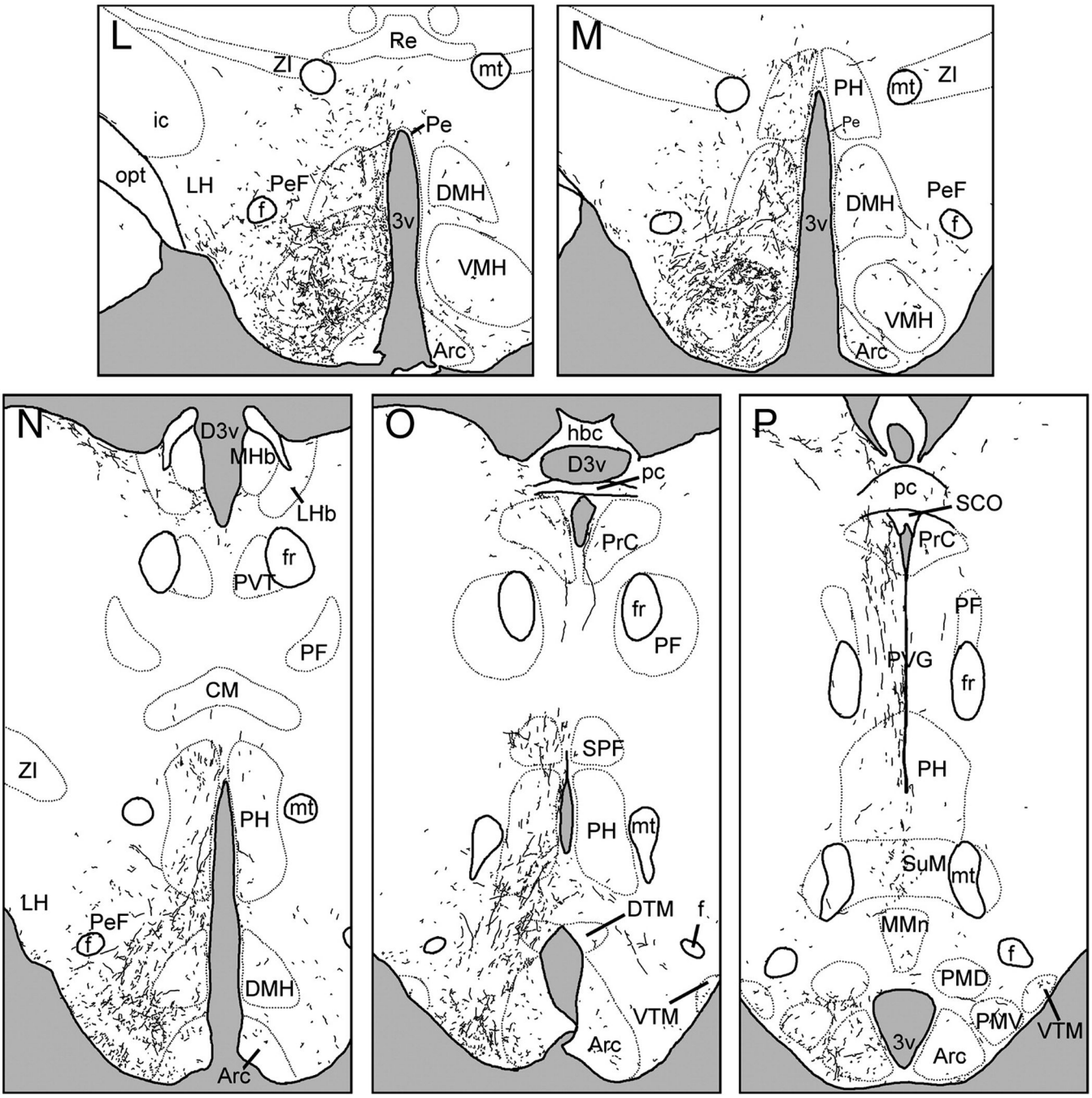

Figure 3.

Line drawings depicting the distribution of BDA- labeled fibers following an injection centered in the ventral subparaventricular zone (VSPVZ; case L1). Panels are arranged rostral-to-caudal, and were traced from sections as described in text. See Table 1 for abbreviations.

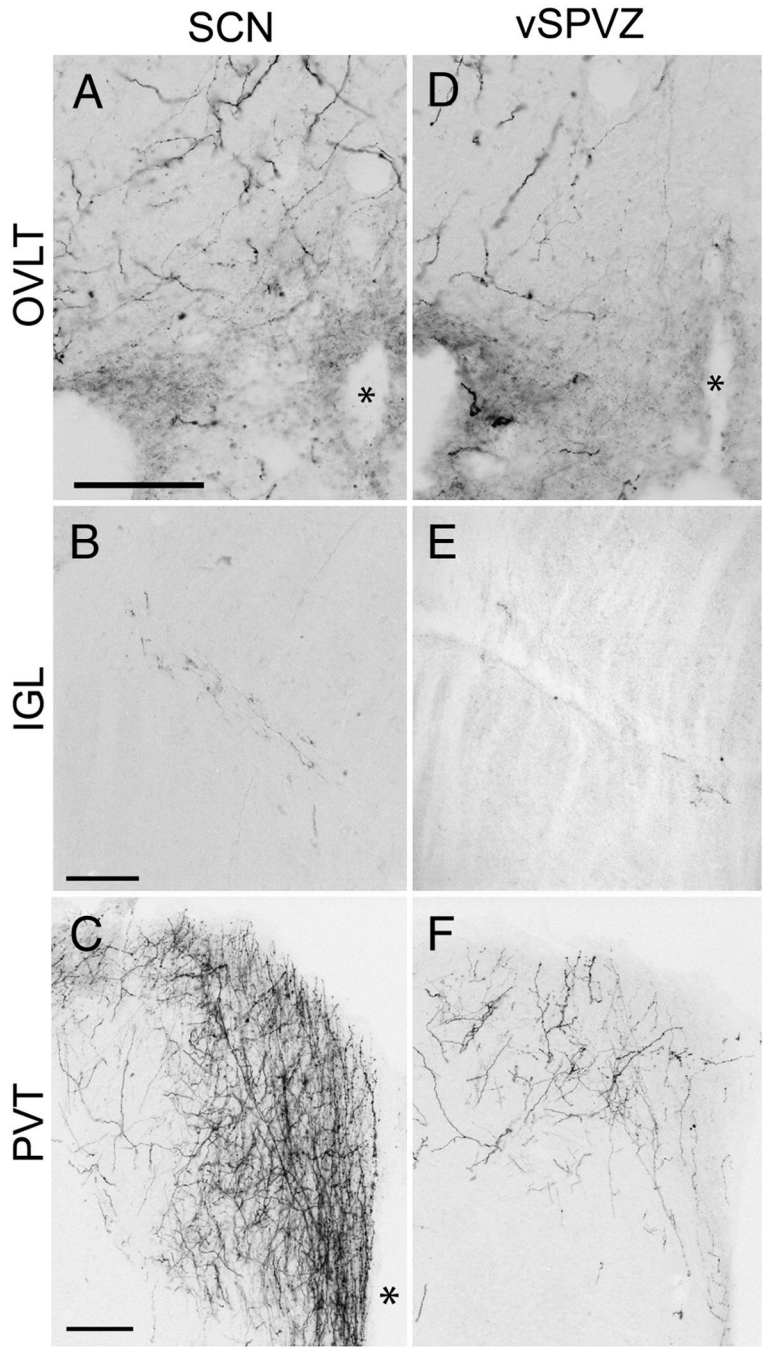

Figure 4.
Photomicrographs of BDA- labeled fibers in the organum vasculosum of the lamina terminalis (OVLT; A, D), intergeniculate leaflet (IGL; B, E), paraventricular thalamic nucleus (PVT; C, F), following BDA injections into the SCN (S1, A–C) and vSPVZ (L3, D–F). * = third ventricle. Scale bar = 100 μm.

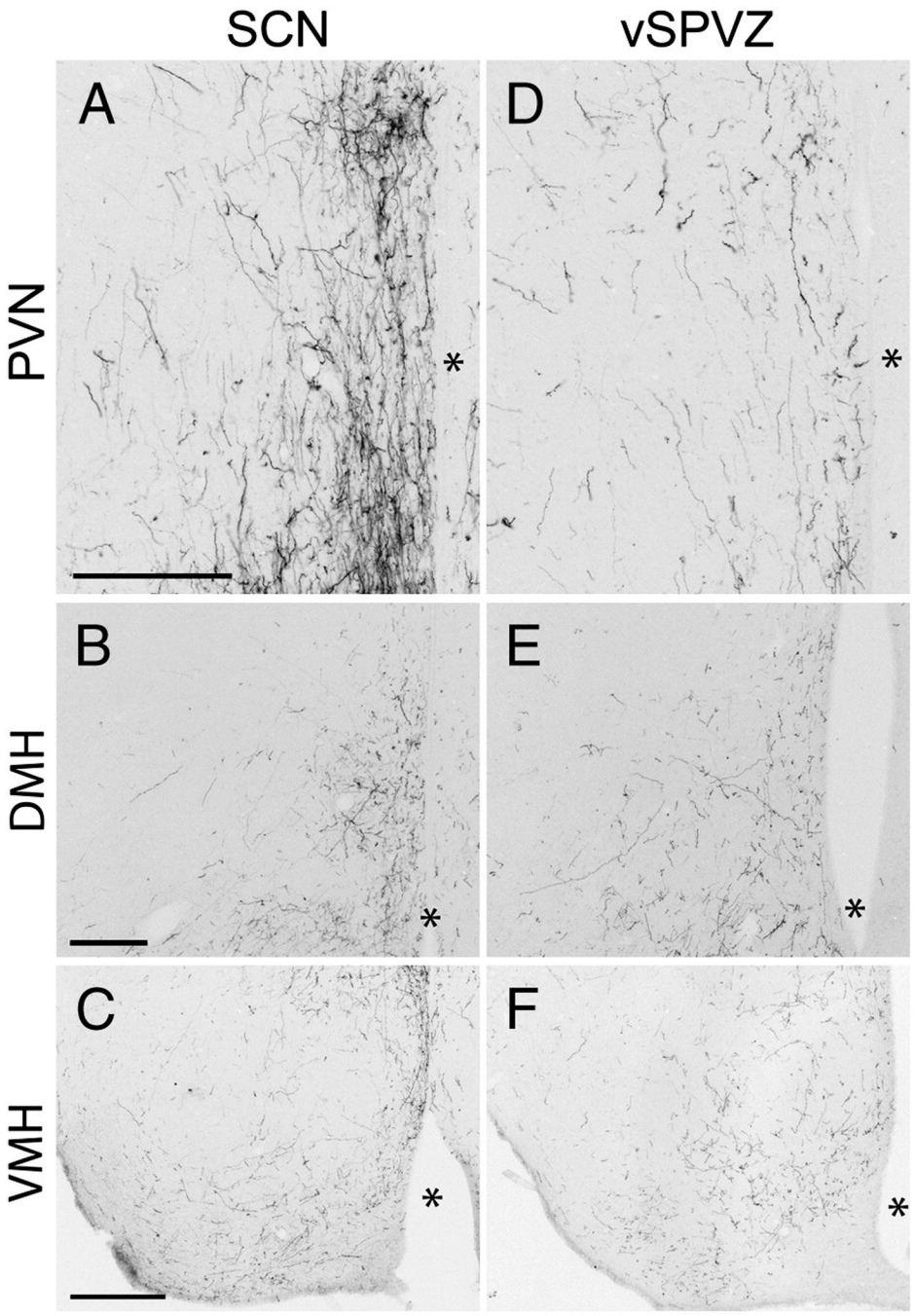

Figure 5.
Photomicrographs of BDA- labeled fibers in the paraventricular hypothalamic nucleus (PVN; A, D); dorsomedial hypothalamus (DMH; B, E) and ventromedial hypothalamus (VMH; C, E) following BDA injections into the SCN (S1, A–C) and vSPVZ (L3, D–F). * = third ventricle. Scale bar = 200 μm (A–B, D–E), 300 μm (C, F).

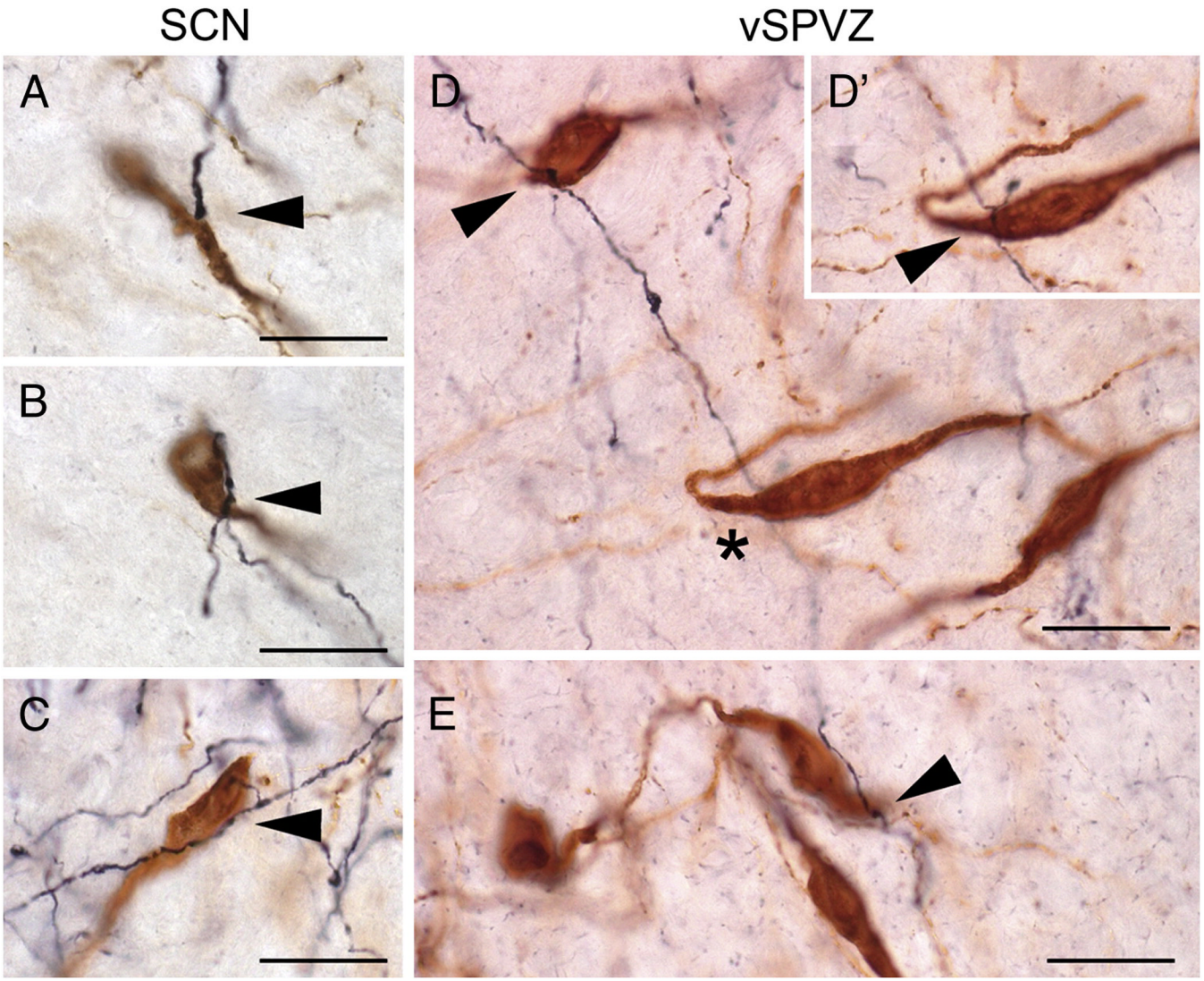

Figure 6.

Photomicrographs of appositions between BDA-ir fibers (black) and GnRH neurons (brown) following injections centered in the SCN (A–C) or vSPVZ (D–E). Appositions, defined as visualization of both GnRH cell and an immediately adjacent BDA-ir fiber in the same plane of focus, are indicated by arrowhead. GnRH neuron and BDA-ir fiber in (D') is the same neuron-fiber pair indicated by an asterisk (*) in (D), with plane of focus adjusted to illustrate apposition. All images were taken using a 100× oil immersion objective. Scale bar = 20 μm.

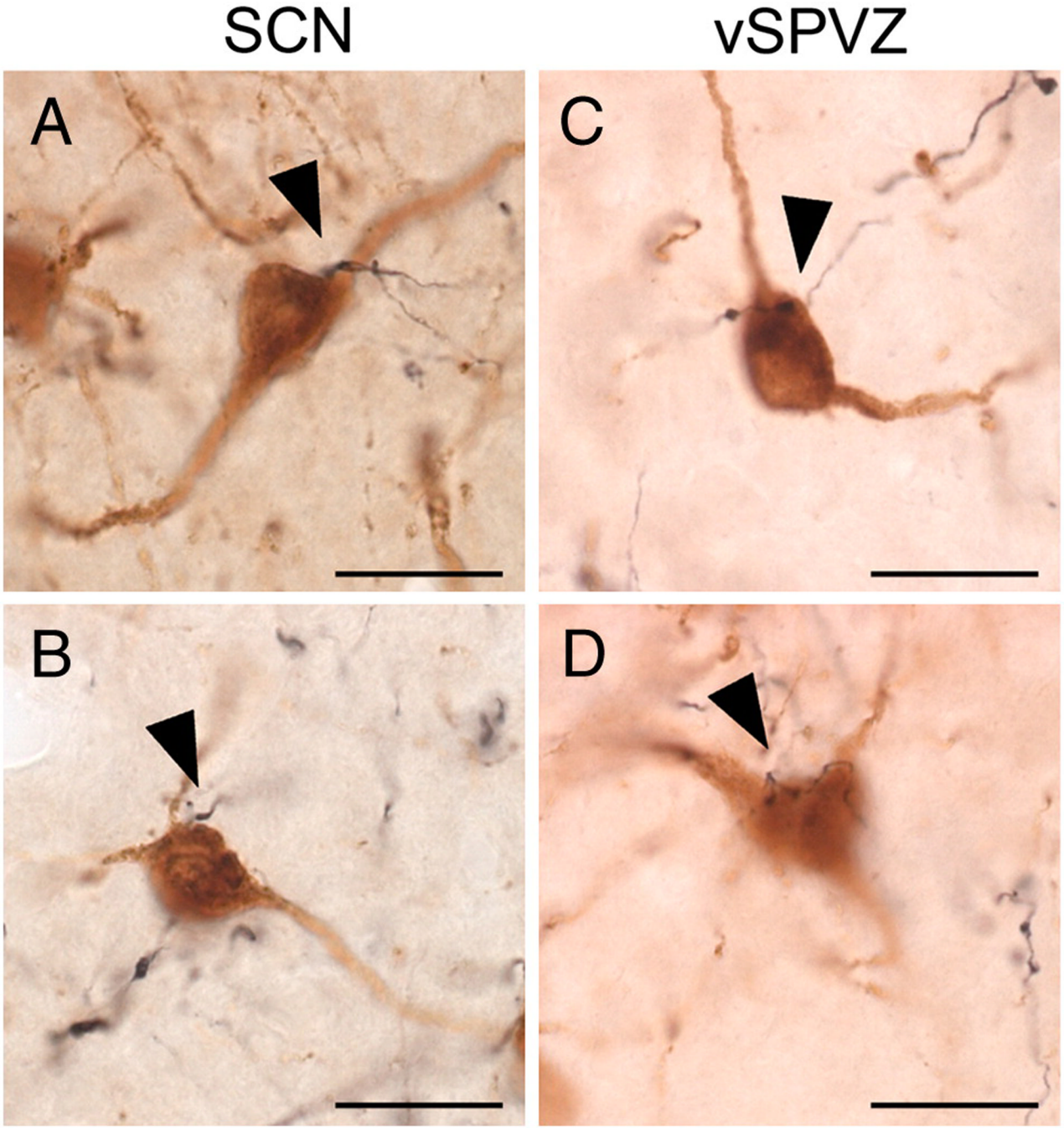

Figure 7.
Photomicrographs of appositions between BDA-ir fibers (black) and OXA neurons (brown) following injections centered in the SCN (A–B) or vSPVZ (C–D). Appositions are defined as in Figure 5, and are indicated by arrowheads. All images were taken using a 100× oil immersion objective. Scale bar = 20 μm.

Table 1

Percentage of GnRH-ir neurons forming appositions with BDA-ir fibers

Percentages of GnRH-ir neurons contacted by BDA-labeled fibers ipsilateral and contralateral to the BDA injection site in each of three regions along the rostrocaudal axis.

Subject		MS/DBB		OVLT		POA/SON	
		ipsi	contra	ipsi	contra	ipsi	contra
SCN	S1	19	32	66	58	51	44
	S2	17	18	55	53	85	58
vSPVZ	L1	27	24	27	27	36	17
	L2	4	17	50	32	69	21
	L3	27	25	44	38	48	35
	L4	22	21	74	28	80	25

Brain Res. Author manuscript; available in PMC 2012 January 7.

Table 2

Percentage of OXA-ir neurons forming appositions with BDA-ir fibers

Percentages of OXA-ir neurons contacted by BDA-labeled fibers ipsilateral and contralateral to the BDA injection site in each of three regions along the medial-lateral axis.

Subject		Medial		Central		Lateral	
		ipsi	contra	ipsi	contra	ipsi	contra
SCN	S1	53	22	11	3	5	4
	S2	89	69	35	12	13	4
vSPVZ	L1	34	2	13	0	9	1
	L2	42	9	24	4	13	3
	L3	50	3	15	1	4	0
	L4	47	4	42	5	31	4